

Transverse energy flow in meson-proton and meson-nucleus interactions at 250 GeV/c

The EHS/NA22 Collaboration

M.R. Atayan⁶, E.A. De Wolf^{1,a}, A.M.F. Endler⁴, Z.Sh. Garutchava⁵, N.G. Grigoryan⁶,
H. Gulkanyan⁶, R. Hakobyan⁶, J.K. Karamyan⁶, W. Kittel³, S. Mehrabyan⁶,
Z.V. Metreveli^{5,b}, F.K. Rizatdinova^{2,c}, E.K. Shabalina^{2,d}, L.N. Smirnova²,
L.A. Tikhonova², A.G. Tomaradze^{5,b}, F. Verbeure¹, S.A. Zotkin²

¹ Department of Physics, Universitaire Instelling Antwerpen, 2610 Wilrijk, Belgium

² Nuclear Physics Institute, Moscow State University, 119899 Moscow, Russia

³ High Energy Physics Institute (HEFIN), University of Nijmegen/NIKHEF, 6525 ED Nijmegen, The Netherlands

⁴ Centro Brasileiro de Pesquisas Fisicas, 22290 Rio de Janeiro, Brazil

⁵ Institute for High Energy Physics of Tbilisi State University, 380086 Tbilisi, Georgia

⁶ Institute of Physics, 375036 Yerevan, Armenia

Received: 7 May 2001 / Revised version: 9 May 2001 /

Published online: 19 July 2001 – © Springer-Verlag / Società Italiana di Fisica 2001

Abstract. The transverse energy carried by charged hadrons and by π^- mesons is studied in interactions of π^+ and K^+ mesons with protons and nuclei at 250 GeV/c. The data obtained on transverse energy flow at mid-rapidity can be described by the FRITIOF7.0 model with tuned parameters.

1 Introduction

In nucleus-nucleus collisions, the transverse energy E_T produced at mid-rapidity serves as a measure of the collision centrality. In order to establish a reliable relation between E_T and the mean impact parameter $\langle b(E_T) \rangle$, information on E_T flow in the ‘elementary’ hadron-nucleon (as well as hadron-nucleus) collisions is needed. The experimental data on E_T production in hadron-nucleon and hadron-nucleus collisions are also necessary to tune event generators used for simulation of the multiparticle production processes. The data on meson-nucleon (meson-nucleus) collisions could, furthermore, be helpful in disentangling the underlying mechanisms in photoproduction reactions.

So far, a small number of calorimetric measurements of the transverse energy production have been performed in pA [1–3], pp and $\bar{p}p$ [4,5], as well as in ep [6,7] collisions. The only data for meson-proton collisions are reported in [5].

In this study, we partially fill a gap in the available data on the transverse energy flow in hadron-nucleon and

hadron-nucleus collisions. To that end, we analyze the data on interactions of π^+ and K^+ mesons with protons and nuclei at 250 GeV/c, collected by the NA22 experiment at the CERN SPS. In Sect. 2 the experimental procedure is described. The data are presented in Sect. 3, compared with predictions of the FRITIOF [8,9] model in Sect. 4, where the model parameters are preliminarily tuned on inclusive spectra of particles produced in non-diffractive π^+p interactions. In Sect. 5, the model predictions are compared with data on proton-nucleus, heavy-ion and photon-proton interactions. The results are summarized in Sect. 6.

2 Experimental procedure

The experiment was performed at CERN in the European Hybrid Spectrometer equipped with the Rapid Cycling Bubble Chamber (RCBC) and exposed to a 250 GeV/c tagged positive meson-enriched beam. The RCBC, filled with liquid hydrogen, was equipped with two nuclear targets consisting of an aluminium and a gold foil of thickness 2.5 mm and 0.64 mm, respectively, corresponding to 0.5% of an interaction length, and placed side by side orthogonally to the beam, 15.5 cm behind the entrance window of the chamber. The experimental setup and the trigger conditions are detailed in [10–13].

Charged-particle momenta are measured over the full solid angle with an average resolution varying from 1-2%

^a Also at CERN, European Organisation for Particle Physics, 1211 Geneva 23, Switzerland

^b Now at Northwestern University, Evanston, USA

^c Now at Kansas State University, Manhattan, KS 66506, USA

^d Now at University of Illinois at Chicago, Chicago, IL 60607, USA

for tracks reconstructed in RCBC and 1-2.5% for tracks reconstructed in the first lever arm, to 1.5% for tracks reconstructed in the full spectrometer. Ionization information is used to identify protons up to 1.2 GeV/c and electrons (positrons) up to 200 MeV/c. All unidentified tracks are given the pion mass, except for the fast ($p > 150$ GeV/c) positive particle in kaon induced reactions, which is given the kaon mass.

The general event selection criteria for interactions in hydrogen and foils are described in [12,13]. Two samples of events are studied. In the first, all charged tracks of an event are required to be properly measured and reconstructed. In the second sample, this requirement is limited to negatively charged tracks. We exclude candidates for elastic scattering and single-diffractive dissociation with charged-particle multiplicity $n \leq 6$ (for meson-proton interactions), as well as candidates for meson-nucleus quasi-elastic or coherent interactions (see details in [6,7]).

The resulting number of selected events N_{tot} is 44956 for $(\pi^+/K^+)p$ interactions for which all tracks are properly reconstructed; 69992 for $(\pi^+/K^+)p$, 3329 for $(\pi^+/K^+)Al$ and 2294 for $(\pi^+/K^+)Au$ interactions for which all negatively charged tracks are properly reconstructed. Each event is given a multiplicity-dependent weight which corrects for the fraction of events excluded due to improperly reconstructed tracks.

For each event, the transverse energy E_T^{ch} carried by charged hadrons (identified pions and unidentified charged particles) and $E_T^{\pi^-}$ carried by negative pions, emitted in a given (pseudo)rapidity window, is calculated as the sum of individual transverse energies $\varepsilon_i \sin \vartheta_i$, where ε_i is the total energy of i -th hadron and ϑ_i is its emission angle in the laboratory frame.

Due to the misidentification of a fraction of charged particles, the values of E_T^{ch} and $E_T^{\pi^-}$ are biased. These biases, estimated by simulations using the FRITIOF7.0 model, result in an overestimation (underestimation) of $\langle E_T^{\text{ch}} \rangle$ ($\langle E_T^{\pi^-} \rangle$) on the average by 2% (0.8%) in the pseudo-rapidity range $1.5 < \eta < 4.5$ and by 5% (6%) in the target fragmentation region ($\eta > 4.5$) the corrections are negligible. The experimental data presented below are not corrected for these biases, since correction would be model dependent, but corresponding biases have been introduced in the model calculations.

Since no statistically significant differences are seen between the results for π^+ and K^+ induced reactions, the two data samples are combined for the purpose of this analysis.

3 Experimental results

3.1 Meson-proton interactions

The dependence of the mean transverse energy $\langle E_T^{\text{ch}} \rangle$ and $\langle E_T^{\pi^-} \rangle$ carried by charged hadrons (mainly π^+ mesons) and by negatively charged hadrons (the overwhelming fraction (93±3)% of which are π^- mesons [14]) on the

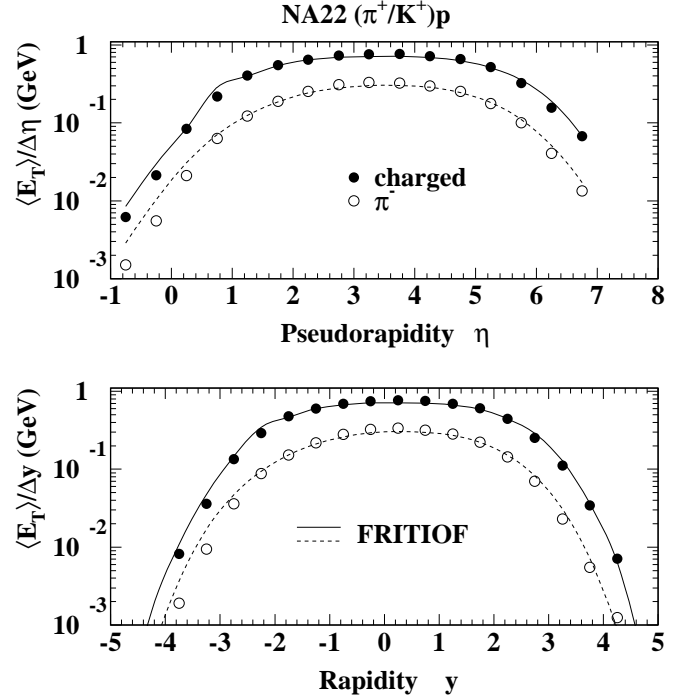


Fig. 1. The pseudorapidity and c.m.s. rapidity dependence of $\langle E_T^{\text{ch}} \rangle$ and $\langle E_T^{\pi^-} \rangle$ in $(\pi^+/K^+)p$ interactions. The full and dashed curves are FRITIOF7.0 predictions for $\langle E_T^{\text{ch}} \rangle$ and $\langle E_T^{\pi^-} \rangle$, respectively

pseudorapidity η and the c.m.s. rapidity y for $(\pi^+/K^+)p$ collisions is plotted in Fig. 1. The maximum transverse energy per unit of (pseudo)rapidity is $\langle E_T^{\text{ch}} \rangle / \Delta\eta \approx \langle E_T^{\text{ch}} \rangle / \Delta y \approx 0.77$ GeV for charged particles and $\langle E_T^{\pi^-} \rangle / \Delta\eta \approx \langle E_T^{\pi^-} \rangle / \Delta y \approx 0.34$ GeV for π^- mesons. In the central rapidity region $-2 < y < 2$ (or, equivalently, $1 < \eta < 5$), the data can be approximated by a Gaussian form of width $\sigma^{\text{ch}} = 2.11 \pm 0.02$ and centroid $y_0^{\text{ch}} = 0.279 \pm 0.010$ for charged particles and $\sigma^{\pi^-} = 1.62 \pm 0.01$ and $y_0^{\pi^-} = 0.267 \pm 0.007$ for π^- mesons (for model comparisons see Sect. 4 below).

The data for fixed charged-particle multiplicity n (and π^- meson multiplicity $n_{\pi^-} = (n-2)/2$) presented in Fig. 2, show that the Gaussian approximation is not valid for the lowest multiplicities ($n \leq 6$). The results of the Gaussian fits for $n \geq 8$ ($n_{\pi^-} \geq 3$) are presented in Tables 1 and 2. With increasing multiplicity, the shape of the distributions narrows significantly, while the maximum tends to converge towards the value of $\eta_c = 3.14$ corresponding to pions with $p_T \gg m_\pi$ emitted at the c.m.s. angle $\vartheta^* = 90^\circ$. The distributions for π^- mesons are narrower, especially at lower multiplicities, than for charged particles. As can be seen from Tables 1 and 2, each additional pair of charged particles (mainly $\pi^+\pi^-$) increases $(d\langle E_T^{\text{ch}} \rangle / d\eta)_{\text{max}}$ on average by 0.27 ± 0.04 GeV, while each π^- increases $(d\langle E_T^{\pi^-} \rangle / d\eta)_{\text{max}}$ on average by 0.12 ± 0.02 GeV, except for the largest multiplicity $n_{\pi^-} = 10$ for which the increase is 0.29 ± 0.06 GeV. These features, inherent to hadron-nucleon collisions, are important when considering the

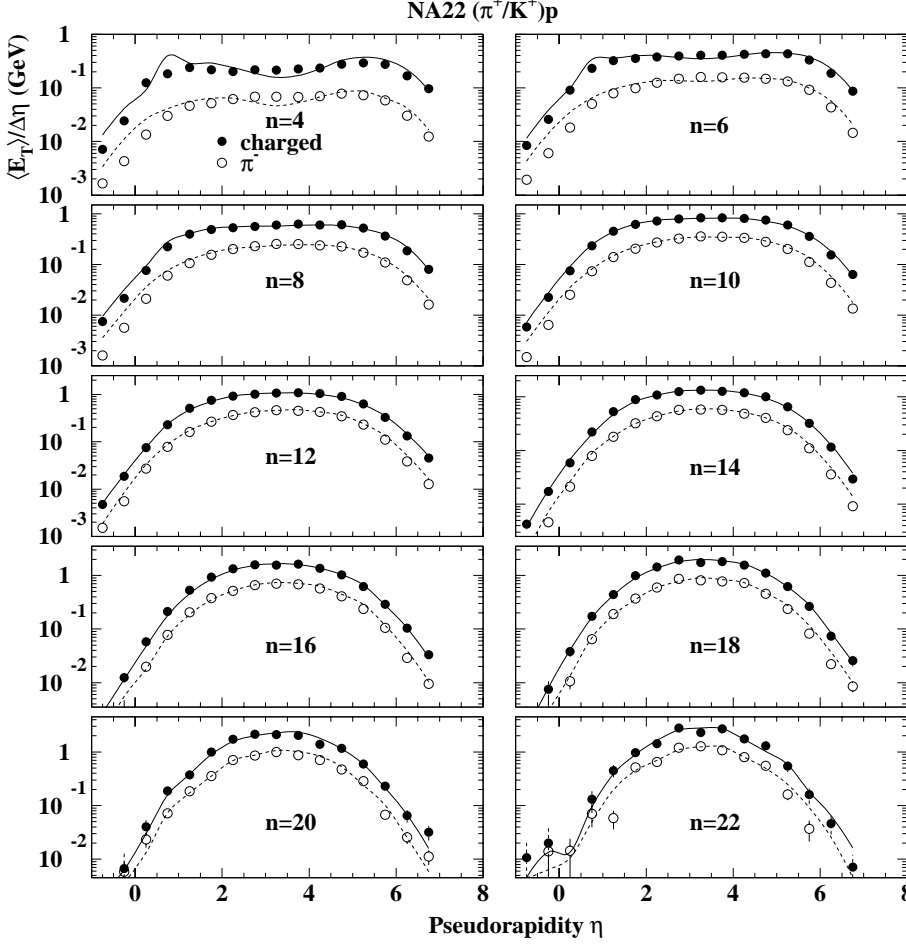


Fig. 2. The pseudorapidity dependence of $\langle E_T^{\text{ch}} \rangle$ and $\langle E_T^{\pi^-} \rangle$ for fixed multiplicities in $(\pi^+ / K^+)p$ interactions. The full and dashed curves are FRITIOF7.0 predictions for $\langle E_T^{\text{ch}} \rangle$ and $\langle E_T^{\pi^-} \rangle$, respectively

Table 1. Results of the Gaussian fit (for $1 < \eta < 5$) of the pseudorapidity dependence of $\langle E_T^{\text{ch}} \rangle$ for different charged-particle multiplicities n for $(\pi^+ / K^+)p$ non-diffractive interactions

n	$(d\langle E_T^{\text{ch}} \rangle / d\eta)_{\text{max}}$ GeV	σ^{ch}	η_0^{ch}
8	0.621 ± 0.004	2.96 ± 0.11	3.97 ± 0.08
10	0.855 ± 0.006	2.14 ± 0.04	3.57 ± 0.03
12	1.102 ± 0.009	1.90 ± 0.04	3.52 ± 0.03
14	1.357 ± 0.014	1.66 ± 0.03	3.42 ± 0.02
16	1.675 ± 0.024	1.41 ± 0.03	3.34 ± 0.02
18	1.950 ± 0.041	1.28 ± 0.03	3.34 ± 0.03
20	2.270 ± 0.083	1.11 ± 0.04	3.28 ± 0.04
22	2.526 ± 0.160	1.15 ± 0.08	3.37 ± 0.07

Table 2. Results of the Gaussian fit (for $1 < \eta < 5$) of the pseudorapidity dependence of $\langle E_T^{\pi^-} \rangle$ for different multiplicities n_{π^-} for $(\pi^+ / K^+)p$ non-diffractive interactions

n_{π^-}	$(d\langle E_T^{\pi^-} \rangle / d\eta)_{\text{max}}$	σ^{π^-}	$\eta_0^{\pi^-}$
3	0.259 ± 0.002	1.87 ± 0.04	3.67 ± 0.03
4	0.362 ± 0.003	1.68 ± 0.03	3.54 ± 0.02
5	0.475 ± 0.004	1.56 ± 0.02	3.48 ± 0.02
6	0.600 ± 0.007	1.43 ± 0.02	3.41 ± 0.02
7	0.717 ± 0.011	1.34 ± 0.03	3.33 ± 0.02
8	0.872 ± 0.020	1.23 ± 0.03	3.35 ± 0.03
9	0.990 ± 0.037	1.14 ± 0.04	3.33 ± 0.04
10	1.280 ± 0.081	0.96 ± 0.04	3.39 ± 0.06

nucleus-nucleus interactions as a superposition of “elementary” nucleon-nucleon collisions.

The distributions $(1/N_{\text{tot}})(dN/dE_T)$ of the transverse energy per event carried by charged and negative particles emitted in the y window of $-1.5 < y < 1.5$ are plotted in Fig. 3. The first (low E_T) point corresponds (mainly) to events for which no charged or no negative particles are produced in that window. The extracted average values

of $\langle E_T \rangle$ are $\langle E_T^{\text{ch}} \rangle = 2.132 \pm 0.007$ GeV and $\langle E_T^{\pi^-} \rangle = 0.892 \pm 0.003$ GeV. The transverse energy carried by positively charged hadrons, $\langle E_T^{\text{pos}} \rangle = \langle E_T^{\text{ch}} \rangle - \langle E_T^{\pi^-} \rangle = 1.24 \pm 0.01$ GeV, is 1.4 times $\langle E_T^{\pi^-} \rangle$.

In view of the current and anticipated investigations of lepton-pair production in nuclear collisions, it is important to have experimental data on the transverse energy $\langle E_T^{\text{ch}} \rangle_a$ carried by charged hadrons accompanying a pair of charged mesons, the main source of background for

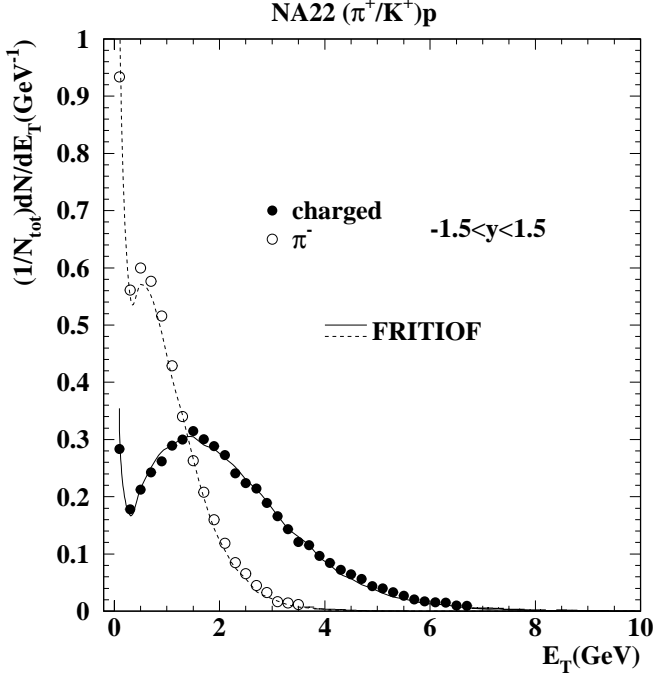


Fig. 3. The E_T^{ch} and $E_T^{\pi^-}$ distributions at mid-rapidity ($-1.5 < y < 1.5$) in $(\pi^+/K^+)p$ interactions. The full and dashed curves are FRITIOF7.0 predictions for E_T^{ch} and $E_T^{\pi^-}$, respectively

dimuons. Figure 4 demonstrates the dependence of $\langle E_T^{\text{ch}} \rangle_a$ (for $1.5 < \eta < 4.5$) on the effective mass $M(\pi\pi)$, the transverse mass $M_T(\pi\pi)$ and the transverse momentum $p_T(\pi\pi)$ of a pair of charged hadrons (mainly $\pi^+\pi^-$, $\pi^+\pi^+$, $\pi^-\pi^-$) emitted into that η window. Note, that the value $\langle E_T^{\text{ch}} \rangle_a$ associated with a pair of negatively charged pions is higher than for $(\pi^+\pi^+)$ and $(\pi^+\pi^-)$ pairs, because events of $n \leq 4$ can contribute to the latter, while $n \geq 6$ holds for the former. Whereas no clear dependence is observed on $M(\pi\pi)$, $\langle E_T^{\text{ch}} \rangle_a$ clearly increases with increasing $p_T(\pi\pi)$. At least for the opposite-sign pair, $\langle E_T^{\text{ch}} \rangle_a$ also tends to rise with increasing $M_T(\pi\pi)$. The observed dependence can induce a small apparent difference in the extracted mean impact parameter for low and high $p_T(M_T)$ dimuons produced in very peripheral nucleus-nucleus collisions, in which only a few nucleons participate.

3.2 Meson-nucleus interactions

The (pseudo)rapidity dependence of $\langle E_T^{\pi^-} \rangle$ produced in collisions with Al and Au nuclei is shown in Fig. 5, where the hydrogen data are repeated for comparison. The nucleus to proton ratio $r_A = \langle E_T^{\pi^-} \rangle_A / \langle E_T^{\pi^-} \rangle_p$ (bottom Fig. 5) continuously increases with decreasing y and reaches $r_{\text{Al}} = 9.5 \pm 1.1$ and $r_{\text{Au}} = 16.3 \pm 1.6$ at $-3.5 < y < -3$, evidencing the essential role of secondary interactions of produced pions in the nucleus. In the beam fragmentation region ($y > 2$), the values of $\langle E_T^{\pi^-} \rangle_{\text{Al}}$ and $\langle E_T^{\pi^-} \rangle_{\text{Au}}$ are almost equal, but smaller than that for meson-proton interactions, especially at larger y ($3 < y < 3.5$), where

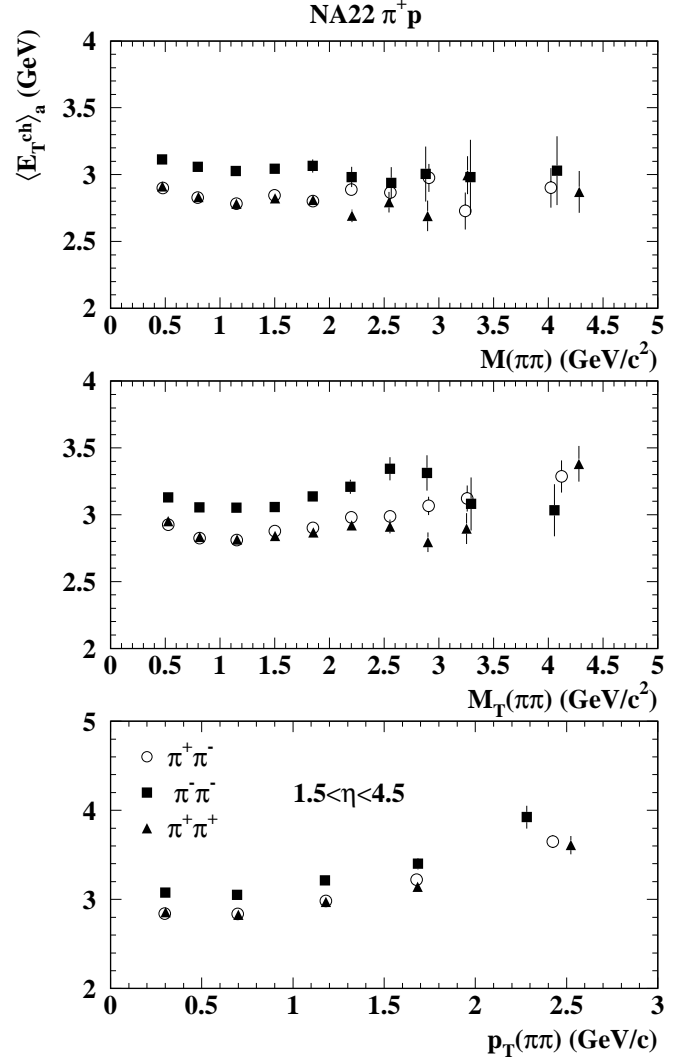


Fig. 4. The dependence of the associated transverse energy $\langle E_T^{\text{ch}} \rangle_a$ on the mass, transverse mass and transverse momentum of an accompanying dipion produced in the window of $1.5 < \eta < 4.5$ in π^+p interactions

$r_{\text{Al}} = 0.29 \pm 0.04$ and $r_{\text{Au}} = 0.34 \pm 0.05$, indicating strong attenuation effects during the passage of the leading projectile (the leading string) through the nucleus. As the mean number of collisions of the leading meson in Al and Au is $\langle \nu_{\text{Al}} \rangle \approx 1.7$ and $\langle \nu_{\text{Au}} \rangle \approx 2.8$ [15], respectively, one can deduce that the attenuation effects influencing $\langle E_T^{\pi^-} \rangle$ ($y > 2$) saturate already after a couple of intranuclear collisions of the leading excited string. Similar features have been observed [15] for the yields $\langle n_{\pi^-} \rangle$ of the high-rapidity π^- mesons.

Mainly due to intranuclear interactions of the produced π^- mesons, the centroid of the Gaussian approximation (for $-2 < y < 2$) of the data plotted in Fig. 5 shifts, with increasing A , towards smaller values, $y_0^{\pi^-}(\text{Al}) = -0.23 \pm 0.04$ and $y_0^{\pi^-}(\text{Au}) = -0.52 \pm 0.05$, as compared to $y_0^{\pi^-}(\text{p}) = +0.267 \pm 0.007$ for meson-proton interactions. Some (minor) role in this shift can be played by the neu-

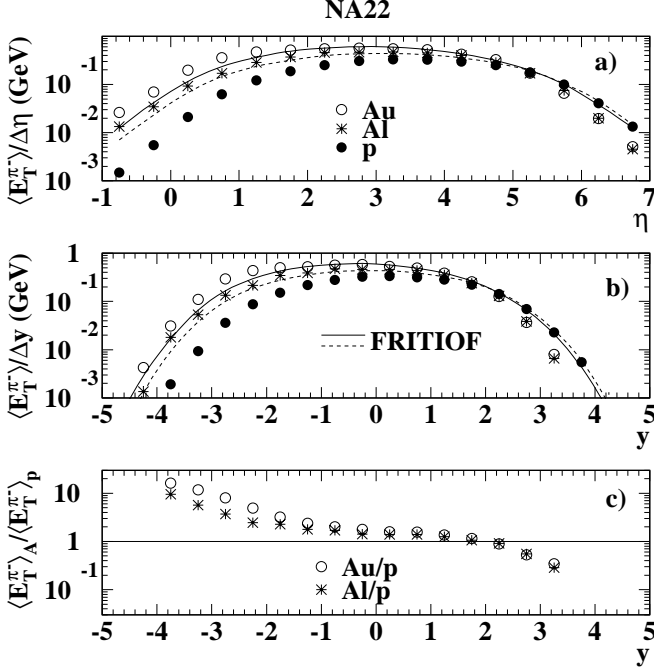


Fig. 5. The pseudorapidity (top) and c.m.s. rapidity (middle) dependence of $\langle E_T^{\pi^-} \rangle$ in (π^+/K^+) interactions with p, Al, Au, and c.m.s. rapidity dependence (bottom) of the nucleus to proton ratio, $\langle E_T^{\pi^-} \rangle_A / \langle E_T^{\pi^-} \rangle_p$. The full and dashed curves are FRITIOF7.0 predictions for Au and Al nuclei, respectively

tron content of the target: neutron fragmentation produces more π^- mesons than proton fragmentation. The fitted widths of the Gaussian approximation, $\sigma_{Al}^{\pi^-} = 1.72 \pm 0.05$ and $\sigma_{Au}^{\pi^-} = 1.82 \pm 0.07$, turn out to be somewhat larger than that for meson-proton interactions ($\sigma^{\pi^-} = 1.62 \pm 0.01$).

The distributions $(1/N_{\text{tot}})(dN/dE_T^{\pi^-})$ in the transverse energy carried by π^- mesons emitted in the window $-1.5 < y < 1.5$ in $(\pi^+/K^+)Al$ and $(\pi^+/K^+)Au$ interactions are plotted in Fig. 6. With increasing A , the distribution widens towards higher $E_T^{\pi^-}$, and its mean value increases from $\langle E_T^{\pi^-} \rangle_p = 0.878 \pm 0.003$ GeV to $\langle E_T^{\pi^-} \rangle_{Al} = 1.31 \pm 0.02$ GeV and $\langle E_T^{\pi^-} \rangle_{Au} = 1.53 \pm 0.03$ GeV. Under the assumption of a power-law parametrization of $\langle E_T^{\pi^-} \rangle_A \sim A^\alpha$, the value of α fitted to the combined hydrogen and nuclear data is $\alpha = 0.11 \pm 0.01$. A fit to the nuclear data alone yields $\alpha = 0.08 \pm 0.01$.

4 Comparison with model predictions

The experimental data are compared with predictions of the FRITIOF7.0 model [8,9]. An important ingredient of the model is the (semi)hard scattering of the partons (mainly gluons) of the colliding hadrons (the Rutherford Parton Scattering, RPS), which was found to be necessary to reproduce the high-multiplicity tail of the charged-particle distribution in high energy hadron collisions. The

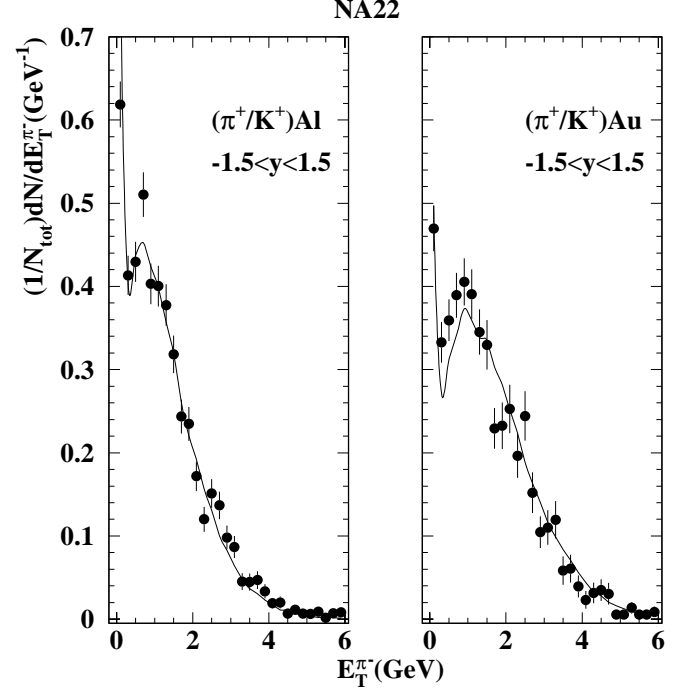


Fig. 6. The $E_T^{\pi^-}$ distribution at mid-rapidity ($-1.5 < y < 1.5$) in $(\pi^+/K^+)Al$ and $(\pi^+/K^+)Au$ interactions. The curves are the FRITIOF7.0 predictions

most essential model parameter which governs the RPS probability is the minimum transverse momentum $q_{T\text{min}}$ acquired by the scattered gluon. Even though still low in the tail, reasonable agreement with the measured multiplicity distribution of non-diffractive π^+p interactions [11, 16] is reached for $q_{T\text{min}} = 0.6$ GeV/ c , as demonstrated in Fig. 7a. The events with $n \leq 6$ satisfying the criteria of the single-diffractive dissociation [16] are excluded both from experimental data and simulated events. Note that for the “default” value of $q_{T\text{min}} = 1$ GeV/ c [9], the model prediction is worse. In the following, we adopted the value $q_{T\text{min}} = 0.6$ GeV/ c .

The model ingredients essentially influencing the predicted transverse momentum distribution of final hadrons are: the distribution of the soft transverse momentum transfer Q_T between the two colliding strings; the distribution of the primordial transverse momentum Q_{2T} carried by the string ends (valence quarks or diquarks) of a string; the distribution of the transverse momentum (p_x and p_y in the string reference frame) acquired by direct (primary) hadrons as a result of string fragmentation. All these distributions are assumed to have a Gaussian form.

The width of the p_x (p_y) distribution is taken from the OPAL setting: $\sigma_x = \sigma_y = 0.37$ GeV/ c [17].

The value of $\langle Q_{2T}^2 \rangle$ adopted in deep inelastic lepton-proton collisions is $\langle Q_{2T}^2 \rangle_{\text{DIS}} = 0.42$ (GeV/ c)² [18,19]. The (semi-hard) hadron-hadron interactions are governed by a larger scale hadron structure corresponding to smaller primordial transverse momentum of valence quarks (diquarks). Hence, smaller values of $\langle Q_{2T}^2 \rangle$ (up to about

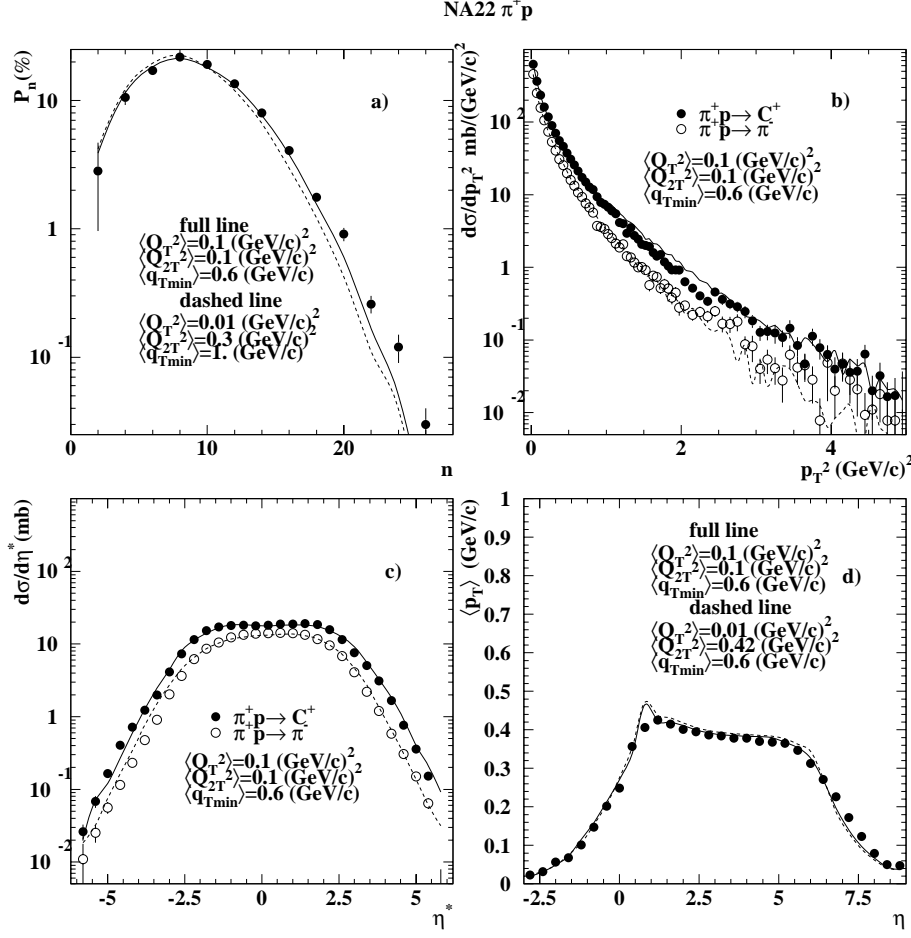


Fig. 7. **a** The charged-particle multiplicity distribution in π^+p interactions. The curves are the FRITIOF7.0 predictions for two different sets of parameters; **b** The p_T^2 distribution for positively charged hadrons C^+ (mainly π^+ and p) and negatively charged hadrons (mainly π^-); FRITIOF7.0: full and dashed lines, respectively; **c** The c.m.s. pseudorapidity distributions for positively and negatively charged hadrons; **d** The η -dependence of the mean transverse momentum for charged hadrons. The curves are FRITIOF7.0 predictions at two different sets of parameters

0.1 (GeV/c) 2) should be used in the model (note, that $\langle Q_{2T}^2 \rangle_{\text{default}} = 0.3$ (GeV/c) 2).

For $\langle Q_T^2 \rangle$ we use a larger value than the “default” one $\langle Q_T^2 \rangle_{\text{default}} = 0.01$ (GeV/c) 2 . Even in single-diffractive scattering the squared transverse momentum acquired by the excited hadron state is $\langle Q_T^2 \rangle_{\text{diff}} = 0.1 - 0.15$ (GeV/c) 2 , while in non-diffractive processes it is $\langle Q_T^2 \rangle_{\text{non-diff}} = 0.1 - 0.4$ (GeV/c) 2 [20, 21].

We tried to tune the parameters $\langle Q_{2T}^2 \rangle$ and $\langle Q_T^2 \rangle$ on the experimental inclusive spectra of positively and negatively charged hadrons produced in non-diffractive π^+p interactions at 250 GeV/c. A reasonable description of p_T^2 and η^* -distributions (Figs. 7b and 7c) is achieved for two sets of parameters (leading to practically indiscernible predictions): $\langle Q_T^2 \rangle = \langle Q_{2T}^2 \rangle = 0.1$ (GeV/c) 2 , and $\langle Q_T^2 \rangle = 0.01$ (GeV/c) 2 , $\langle Q_{2T}^2 \rangle = 0.42$ (GeV/c) 2 . A slightly better description of the η -dependence of the mean transverse momentum of charged hadrons (Fig. 7d) is provided by the first set of parameters, which are finally chosen for comparison with the transverse energy spectra.

With tuned parameters, the model describes satisfactorily the transverse energy data in $(\pi^+/K^+)p$ collisions (Figs. 1–3), only slightly underestimating the data in the central (pseudo)rapidity region. This underestimation holds also for $(\pi^+/K^+)Al$ data, while better agreement in the central (pseudo)rapidity region is achieved for $(\pi^+/$

$K^+)Au$ data (Fig. 5). Since secondary intranuclear interactions of the produced hadrons are not included in the model, is unable to reproduce the enhanced transverse energy flow in the target fragmentation region ($\eta < 1$ or $y < -2$), especially for the case of the (heavier) Au target. The model also overestimates the data in the beam fragmentation region ($\eta > 5$ or $y > 2$), which can be caused by an underestimation of the multiple scattering effects during the passage of the leading string through the nucleus. Nevertheless, the model reproduces well the $E_T^{\pi^-}$ distribution at mid-rapidity ($-1.5 < y < 1.5$) for meson-nucleus interactions (Fig. 6).

In so far as the FRITIOF7.0 model provides a satisfactory description of hadronic interactions, its predictions for hadron-nucleus and heavy-ion collisions can, in a comparison with experimental data, serve as a reference for a quantitative estimation of secondary intranuclear collision effects.

5 Comparison with other data

The FRITIOF7.0 predictions obtained with the same parameters as used in Sect. 4, have been compared in Figs. 8 and 9a with the η -dependence of the transverse energy E_T at different centralities of proton-nucleus [3] and heavy-ion

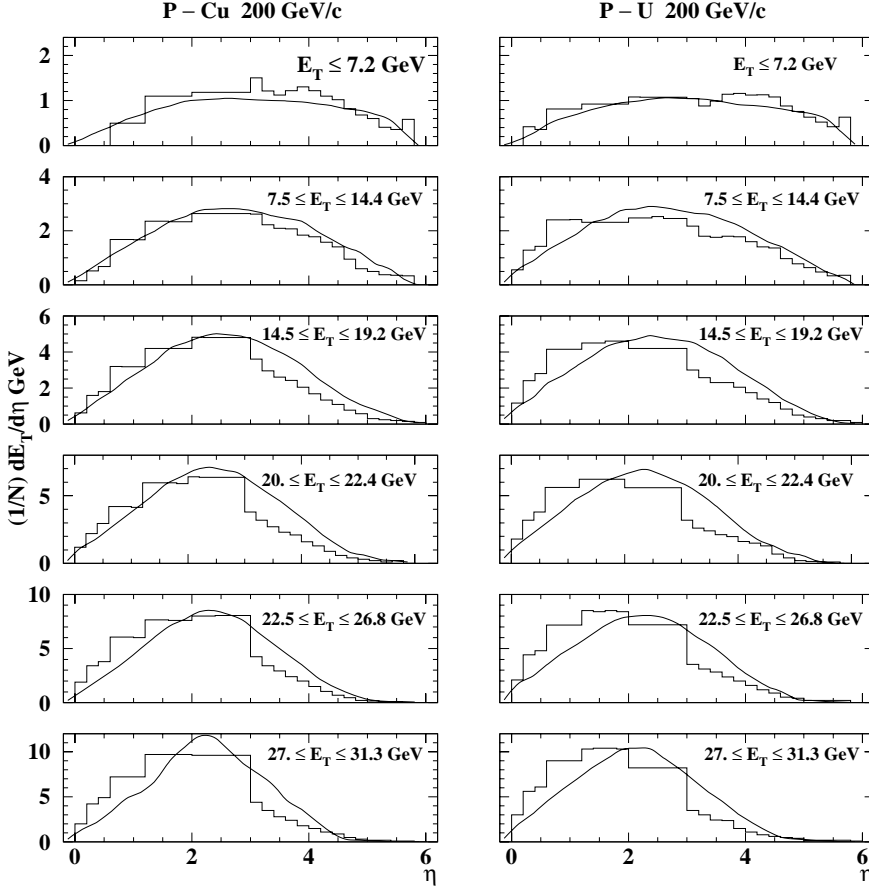


Fig. 8. The pseudorapidity dependence of E_T in pCu and pU interactions at 200 GeV/c in different E_T slices. The curves are FRITIOF7.0 predictions

[22] collisions. The simulated events are selected according to appropriate experimental trigger conditions. A comparison with pCu and pU interactions at 200 GeV [3] is shown in Fig. 8. For non-central collisions ($E_T \leq 14.4$ GeV), which comprise a large fraction of cross section (84% for pCu and 66% for pU interactions), the model qualitatively reproduces the data (taking into account 8% systematical errors in the data [3]). For central collisions ($E_T \geq 14.5$ GeV), the model fails in describing the data in the target fragmentation region (especially for the heavier nucleus) and in the region $\eta > 3$. However, the predictions for the transverse energy emitted in a restricted mid-rapidity region, $1.9 < \eta < 2.9$, agree with the data within an accuracy of about 10% for Cu and about 15% for U.

The comparison with 200A GeV S+Au data shows (Fig. 9a), that the model qualitatively reproduces the data for peripheral collisions ($7 < b < 11.5$ fm) in a wide η -range, as well as the data for intermediate centralities ($3.8 < b < 7$ fm) in the mid-rapidity range of $1.7 < \eta < 3$. As is the case of pA collisions, the model fails in describing the data for $\eta > 3$, especially for the most central collisions ($b < 3.8$ fm).

Finally, we compare the model predictions for π^\pm p collisions with the photoproduction data [6] on $dE_T/d\eta^*$ at HERA energies ($\sqrt{s} = W \approx 180$ GeV) and with the deep-inelastic scattering results for virtual-photon proton collisions (mean virtuality $Q^2 = 3.5$ GeV²) [7] plotted in Fig. 9, where η^* is defined in the hadronic c.m.s., negative

values of η^* now corresponding to the photon (pion) fragmentation region. Despite non-negligible systematic errors in the data (varying from 8–9% for $\eta^* > -3.5$ up to 20% for $\eta^* < -3.5$) for photoproduction, a clear shift toward larger η^* is seen of the model predictions as compared to the HERA data.

6 Summary

New experimental results are presented on the mean transverse energy, $\langle E_T^{\text{ch}} \rangle$, carried by charged hadrons in (π^+/K^+)p interactions and the transverse energy ($E_T^{\pi^-}$) carried by negative hadrons in collisions of (π^+/K^+) mesons with hydrogen, aluminium and gold nuclei at 250 GeV/c. The (pseudo-)rapidity dependence of $\langle E_T^{\text{ch}} \rangle$ and $\langle E_T^{\pi^-} \rangle$ in the whole (pseudo)rapidity range, as well as the distributions of E_T^{ch} and $E_T^{\pi^-}$ for particles emitted at mid-rapidity are measured. The dependence of $\langle E_T^{\text{ch}} \rangle$ on the multiplicity n of charged particles and on the kinematical variables of an associated hadron pair is studied. It is shown that $\langle E_T^{\text{ch}} \rangle$ at mid-rapidity increases almost linearly with increasing n : for $n > 6$, each additional produced hadron pair increases the maximum transverse energy density, $(dE_T^{\text{ch}}/dy)_{\text{max}}$, on average by 0.27 ± 0.01 GeV. The mean transverse energy carried by charged hadrons accompanying a “trigger” dimeson with small transverse momentum (< 0.5 GeV/c)

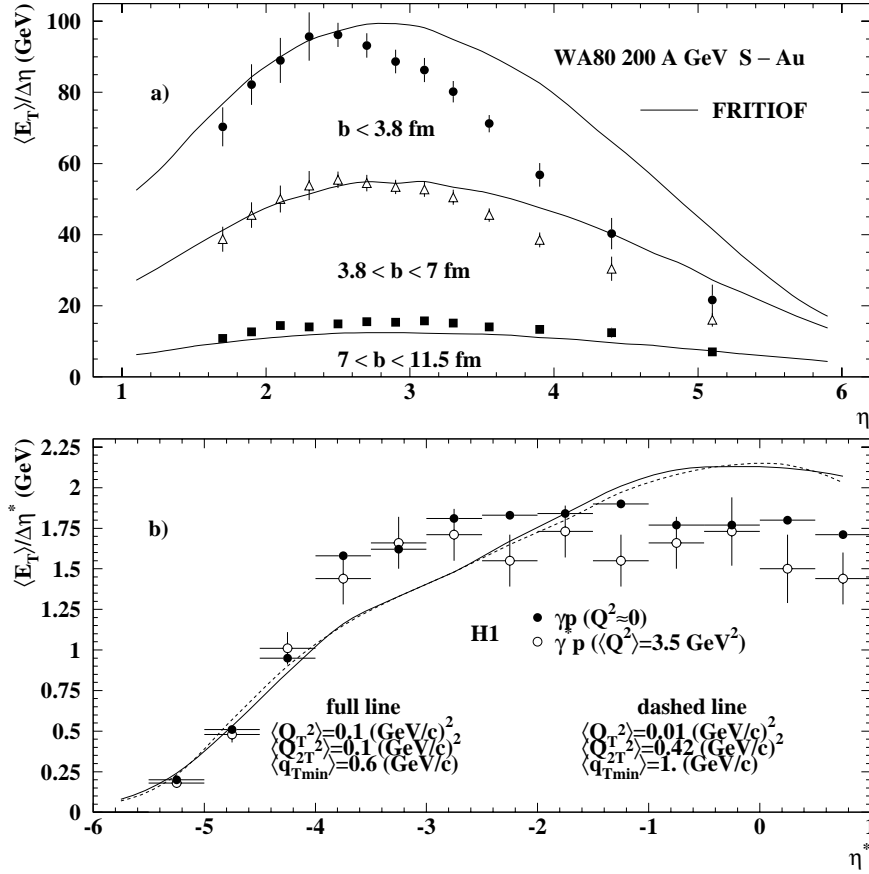


Fig. 9. **a** The pseudo-rapidity dependence of the transverse energy at different centralities of 200A S+Au collisions as compared to FRITIOF7.0 predictions (the curves). **b** The pseudo-rapidity dependence of the transverse energy in the hadronic c.m.s. in γp interactions at $W \approx 180$ GeV and $\gamma^* p$ at HERA, compared to FRITIOF7.0 predictions for πp interactions (the curves)

is smaller by about 30% than for the case of a high p_T (>2 GeV/c) “trigger” meson; this fact should be taken into account when extracting the mean impact parameter (corresponding the measured value of E_T) in very peripheral nucleus-nucleus collisions.

The influence of nuclear effects on the $\langle E_T^{\pi^-} \rangle$ production at mid-rapidity and in the target and beam fragmentation regions is investigated. This influence is maximal in the target fragmentation region, being reduced with increasing (pseudo)rapidity and being almost the same for the light (Al) and heavy (Au) nuclei at the largest (pseudo)rapidities. At mid-rapidity, the maximum value of $\langle E_T^{\pi^-} \rangle$ per unit rapidity varies from 0.337 ± 0.001 GeV for meson-proton interactions to 0.49 ± 0.01 and 0.59 ± 0.01 GeV for meson-aluminium and meson-gold interactions, respectively.

The data are compared with predictions of the FRITIOF7.0 model with parameters tuned on inclusive spectra of positively and negatively charged particles produced in non-diffractive $\pi^+ p$ interactions at 250 GeV/c. The model describes well the data on $\langle E_T^{\text{ch}} \rangle$ and $\langle E_T^{\pi^-} \rangle$ for meson-proton interactions, as well as on $\langle E_{\pi^-} \rangle$ at mid-rapidity in meson-nucleus interactions. The model qualitatively reproduces the data on E_T in peripheral proton-nucleus and heavy-ion collisions, but fails for more central ones. The comparison of the model predictions for higher energy πp interactions ($\sqrt{s}=180$ GeV) with the H1 photoproduction and deep-inelastic data reveals a similarity

in the photon and pion fragmentation ($\eta^* < -4$), but the model fails at larger η^* ($-4 < \eta^* < 1$).

Acknowledgements. We are grateful to the III. Physikalisches Institut B, RWTH Aachen, Germany, the DESY-Institut für Hochenergiephysik, Berlin-Zeuthen, Germany; the Department of High Energy Physics, Helsinki University, Finland; the Institute of Physics and Nuclear Techniques of the Academy of Mining and Metallurgy and the Institute of Nuclear Physics, Krakow, Poland; the Institute for High Energy Physics, Protvino, Russia; and the University of Warsaw and Institute of Nuclear Problems, Poland for their contributions to this experiment. This work is part of the research program of the “Stichting voor Fundamenteel Onderzoek der Materie (FOM)”, which is financially supported by the “Nederlandse Organisatie voor Wetenschappelijk Onderzoek (NWO)”. We further thank NWO for support of this project within the program for subsistence to the former Soviet Union (07-13-038). The Yerevan group activity is financially supported, in the framework of the theme No. 01-183, by the Government of the Republic of Armenia.

References

1. T. Åkesson et al., HELIOS Coll.: Nucl. Phys. A **447** (1985) 475c
2. R. Gomez et al., E-557 Coll.: Preprint FERMILAB-Conf. 86/85-E

3. T. Åkesson et al., HELIOS Coll.: *Z. Phys. C* **58** (1993) 239
4. C. Albajar et al., UA1 Coll.: *Nucl. Phys. B* **335** (1990) 261
5. A. De Roeck: Inclusive Particle Production in Hadron-Proton Interactions at 250 GeV/c. Ph. D. Thesis, Antwerpen (1988), unpublished
6. S. Aid et al., H1 Coll.: *Phys. Lett. B* **358** (1995) 412
7. C. Adloff et al., H1 Coll.: *Eur. Phys. J. C* **12** (2000) 595
8. B. Andersson, G. Gustafson, *Hong Pi*: *Z. Phys. C* **57** (1993) 485
9. *Hong Pi*: *Comput. Phys. Commun.* **71** (1992) 173
10. M. Aguillar-Benitez et al.: *Nucl. Instrum. Methods* **205** (1983) 79
11. M. Adamus et al., NA22 Coll.: *Z. Phys. C* **32** (1986) 475
12. M. Adamus et al., NA22 Coll.: *Z. Phys. C* **39** (1988) 311
13. I. V. Ajinenko et al., NA22 Coll.: *Z. Phys. C* **42** (1989) 377
14. M. Adamus et al., NA22 Coll.: *Z. Phys. C* **33** (1988) 301
15. N. M. Agababyan et al., NA22 Coll.: *Z. Phys. C* **56** (1992) 371
16. M. Adamus et al., NA22 Coll.: *Z. Phys. C* **39** (1988) 301
17. M. Z. Akrawy et al.: *Z. Phys. C* **47** (1990) 505
18. M. Arneodo et al.: *Phys. Lett. B* **149** (1984) 415
19. M. Arneodo et al.: *Z. Phys. C* **36** (1987) 527
20. I. V. Ajinenko et al., NA22 Coll.: *Z. Phys. C* **49** (1991) 367
21. N. M. Agababyan et al., NA22 Coll.: *Z. Phys. C* **75** (1996) 229
22. A. Albrecht et al., WA80 Coll.: *Phys. Rev. C* **44** (1991) 2736